Trends in Renewable Energy
OPEN ACCESS ISSN: 2376-2144
Peer-Reviewed Article futureenergysp.com/index.php/tre

Mechanical Study of a Solar Central Air Conditioning Duct Cleaning Robot

Li Sun*

School of Mechanical Engineering, North China University of Water Resources and Electric Power, Zhengzhou, Henan 450045, CHINA

Received May 30, 2024; Accepted June 29, 2024; Published July 10, 2024

With the rapid economic development and the depletion of fossil fuels, the use of renewable energy such as solar energy can help alleviate energy supply pressure and carbon emissions. There have been many studies on solar energy powered robots. In this paper, a solar-powered duct-cleaning robot is used as the basis for the design of its mechanism. The robot is designed to clean vertical ducts with a length of 5~10 meters, a width of more than 400 mm and a height of 500~800 mm. The design of the robot is based on four aspects: solar energy, drive, camera and cleaning device. AutoCAD was used for 2D drawing of each part, while SolidWorks was used for modeling and assembling the parts of the vertical duct cleaning robot. The solar duct cleaning robot is characterized by high adaptability, low cost, and smooth and fast movement within the allowed size range.

Keywords: Vertical ventilation ducts; Solar energy; Cleaning robot; AutoCAD; SolidWorks

Introduction

Since entering the 21st century, the demand for energy has increased dramatically. However, with the gradual reduction of fossil energy reserves and the current deterioration of the environment, finding new energy sources and energy conservation and emission reduction have become urgent issues that need to be addressed by all countries. Taking several current new energy sources into consideration, solar energy has more prominent advantages. It is not only abundant in resources and widely distributed, but also has zero emissions. The installed capacity is increasing year by year, and it is the mainstream of current new energy development [1]. In the development of the photovoltaic (PV) industry, with the continuous advancement of global industrialization, the photovoltaic industry has gradually gained good market and economic support. It is predicted that by around 2050, photovoltaic power generation is expected to reach 10% to 20% of the electricity supply, becoming an indispensable part of the human energy structure [2]. Since 1970, a global upsurge in photovoltaic power generation technology research has emerged, and corresponding industrial planning has been formulated. Through various promotions, the rapid development of the photovoltaic industry has been promoted [3]. As one of the fastest growing industries today, the photovoltaic industry has immeasurable potential for future development.

The formal research on solar cars began in the UK. In 1978, the world's first solar car was born in the UK, with a speed of up to 13 km/h. In 1982, Mexico's three-wheeled

*Corresponding author: 2362911483@qq.com

Tr Ren Energy, 2024, Vol.10, No.2, 239-256. doi: 10.17737/tre.2024.10.2.00175

solar car could reach a speed of 40 km/h, but its range was only 40 minutes. Ahmed *et al.* [4] analyzed lightweight solar vehicles from an economic perspective and the results showed that the total cost of lightweight solar vehicles over their service life is much lower than that of traditional vehicles. Alhammad *et al.* [5] investigated ways to improve the conversion efficiency of PV modules and used it as an auxiliary power source for a light-storage hybrid solar car. Tang *et al.* [6] analyzed the feasibility of photovoltaic electric vehicles from both technical and economic perspectives. The research results show that the energy cost of photovoltaic electric vehicles is USD$0.204/kWh to $0.372/kWh, which is higher than that of grid-connected electric vehicles ($0.150/kWh), but greenhouse gas emissions can be reduced by 47%-78%. Photovoltaic electric vehicles are considered to be the most promising model in the near future. Selin *et al.* [7] conducted in-depth research on the energy usage of solar racing cars on fixed routes and implemented it in the SPbPUStrat software solution, which greatly improved the utilization rate of solar energy and increased the chances of success. This study combines solar energy with a cleaning robot, and the design can have many advantages such as energy saving and environmental protection, long driving range, relatively mature technology, simple transformation, short development cycle, and superior performance.

The central air conditioning system dominates the air circulation and exchange within the building, so it is also known as the “lungs of the building” [8]. However, its own “health” is not optimistic. The central air conditioner that has not been cleaned for a long time is much dirtier than you think: Studies have shown that an air conditioner heat exchanger that has not been cleaned for three years contains 230 g of dust, 56 g of flakes, and 15 g of oil smoke. The number of bacteria can be up to 60 times that of a toilet bowl [9]. If the inner wall of the duct is only cleaned by ordinary means, it is difficult to clean it thoroughly [10]. As the epidemic has become normalized, it is also required to disinfect the inner walls of air-conditioning ducts. However, the cleaning and maintenance of central air-conditioning is very inconvenient for people, whether it is household air-conditioning or air-conditioning in public buildings [11]. There are three main hazards of not cleaning the central air conditioner for a long time: First, due to the lack of ventilation and gas exchange with the outside world for a long time, the dust accumulated indoors will increase, causing people working indoors to be infected with viruses; Second, dust and foul-smelling gases will remain in the air; Third, people will suffer from "Legionnaires' disease" (Figure 1). Therefore, the cleaning and disinfection of central air-conditioning ventilation ducts requires sufficiently advanced cleaning and disinfection equipment, and the invention and manufacture of duct cleaning robots is a historical choice.

The cleaning of ventilation ducts is to divide the ducts into several sections, open a window in each section, and use the high-speed rotation of the cleaning mechanism to drive the brush on the telescopic arm to brush off the dust adhering to the inner wall. After brushing, use a vacuum cleaner to suck out the stubborn dust, thereby achieving the purpose of cleaning the inner wall of the duct. The cleaning process is shown in Figure 2 [12].

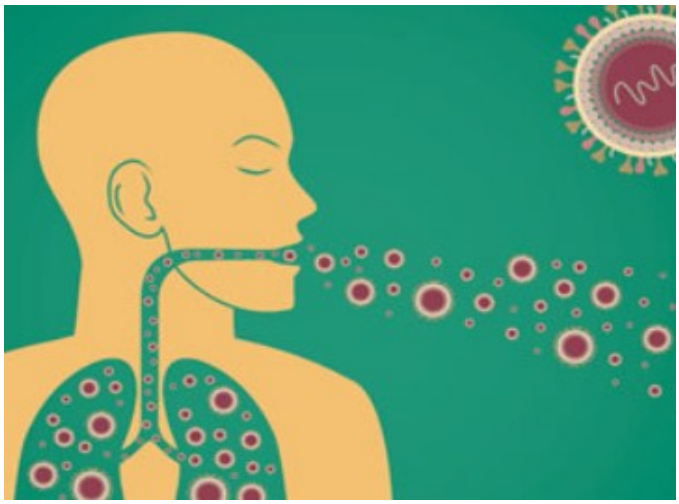

Fig. 1. Schematic diagram of the respiratory system infected with Legionella

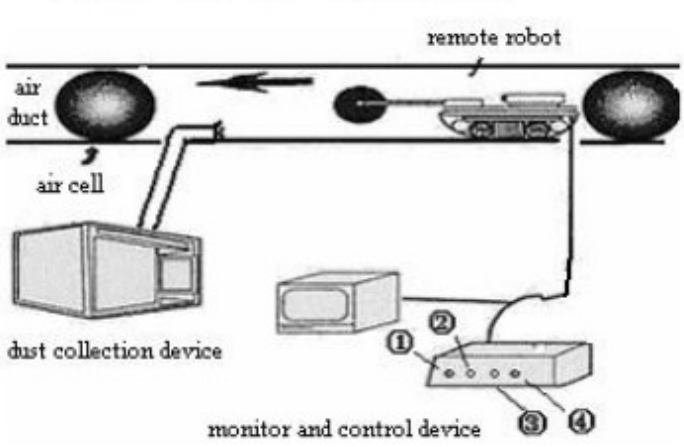

Fig. 2. Workflow diagram of duct cleaning robot [12]

The traditional cleaning robot does not realize the function of intelligent work, and is not very targeted, and there is no special device for a specific working environment. The cleaning robot designed in this paper has a simple structure and light weight, which is conducive to the subsequent addition of solar energy devices. It mainly cleans the vertical direction of the central air-conditioning ventilation duct and related structural design to achieve efficient cleaning of the vertical duct.

Overall Design of Duct Cleaning Robot

The design of the central air conditioning vertical duct cleaning robot in this paper is divided into four main parts: wheeled mobile mechanism design, flexible arm cleaning mechanism design, camera lighting device and solar power generation system design.

(1) The cleaning robot adopts a wheeled moving mechanism, which has stronger adaptability than other mechanisms. It uses the suction cup on the body for positioning when moving, and the positioning of the cleaning robot on the inner wall of the duct is achieved by evacuating the air between the suction cup and the inner wall of the duct.

(2) As for the cleaning mechanism of the cleaning robot, it mainly drives the cleaning mechanism with bristles of different sizes through a driving motor to complete the cleaning work of the vertical ventilation duct at high speed.

(3) During the cleaning operation, it is impossible to complete the cleaning task successfully every time, so the operator needs to develop corresponding solutions according to different working conditions. Therefore, it is necessary to equip a CCD camera and lighting equipment. The CCD camera transmits the signal to the display in front of the operator through a matching cable so that the operator can make corresponding solutions [13].

(4) Solar cells convert solar energy into the electricity needed by the machine, ensuring the robot's battery life and making work more environmentally friendly.

Selection of Drive Motors for Mobile Mechanisms

The selected motor should have the following characteristics: fast response, multi-stage speed regulation, small torque fluctuation, small size and light weight. DC motors have the advantages of a wide speed regulation range, good smoothness, and strong overload capacity. Therefore, this robot chooses DC reduction motors (Figure 3) as the driving mode of the mobile mechanism [14].

Fig. 3. Schematic diagram of DC geared motor

The resistance F encountered by the duct cleaning robot when cleaning in a vertical duct is:

$$F=aG+G+F_1 \quad \text{Eq. 1}$$

where a is the rolling resistance coefficient between the ducts, which is taken as 0.014; the self-weight of the robot is G, and the resistance generated by the load carried is F_1; and the gravitational acceleration g=10 m/s^2.

The total resistance F_2 is:

$$F_2 = K \times F \quad \text{Eq. 2}$$

where K is the resistance correction factor; k = 1.2.

Assuming that the self-weight of the duct cleaning robot is 10 kg and the resistance generated by the load it carries is 3 kg, the resistance F of the duct cleaning robot as it proceeds through the vertical duct is:

$$F = 1.014G + F_1 = 131.4N \quad \text{Eq. 3}$$

Total resistance is:

$F_2 = K \times F = 158N$ Eq. 4

The drag force on each drive wheel is:

$F_3 = \frac{F_2}{2} = 79N$ Eq. 5

Let the maximum speed of the duct cleaning robot be 12 m/min then:

$P = F \times V = 15.8W$ Eq. 6

Check the table to take the working condition factor $K_a = 1.6$:

$P = K_a \times P = 25.28W$ Eq. 7

The maximum speed of the wheel is:

$n = \frac{V}{\pi} \times d = 12/3.14 \times 0.13$ Eq. 8

Drive motor: According to the calculated power and speed, select a DC gear motor with a rated power of 30 W and a rated voltage of 24 V.

Wheel Strength Check

The wheels are the most stressed part of the entire mechanism and are the guarantee for the robot to work properly. Therefore, we need to consider the material of the wheel and whether the strength of the wheel is sufficient for the work of this project. Considering both economic and strength requirements, 45 steel is selected as the wheel material. At the same time, in order to reduce the risk of the robot slipping during work, the roller surface is knurled to increase the friction during processing.

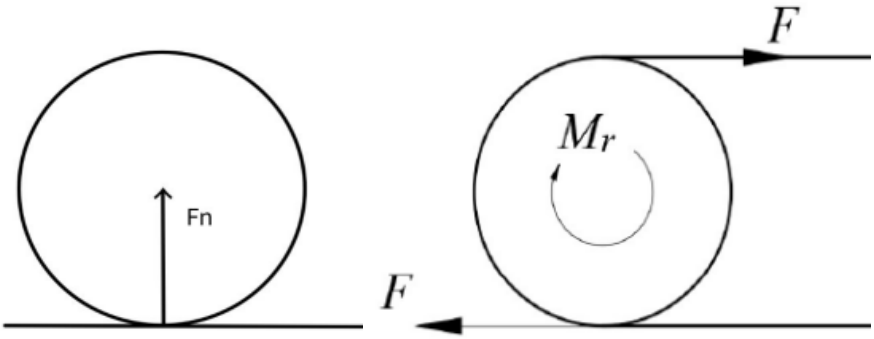

Fig. 4. Sketch of the forces on the wheels

In Figure 4, $M\mathbf{r}$ is the output torque of the motor, and F is the force imparted to the wheel by the rotation of the motor, which offsets the torque:

Rated torque of the motor: $0.4N \cdot \mathbf{m}$

Reducer reduction ratio: i=100

Transmission efficiency: $\boldsymbol{\eta}$ =0.7

$M\mathbf{r} = \mathbf{i} \times \boldsymbol{\eta} \times M = \mathbf{100} \times \mathbf{0}.7 \times \mathbf{0}.\mathbf{4} = \mathbf{28}N \cdot \mathbf{m}$ Eq. 9

From moment equilibrium:

$M\mathbf{r} = \mathbf{2F} \times d/2$ Eq. 10

Then the magnitude of the force on the wheel in the horizontal direction is:

$F = \frac{M\mathbf{r}}{\mathbf{d}} = \mathbf{215N}$ Eq. 11

The magnitude of the force on the wheel in the vertical direction is:

$F_n = G + F_1 = 130N$ Eq. 12

The force in the vertical direction on each wheel is:

$$F = \frac{F_n}{4} = 32.5N \quad \text{Eq. 13}$$

As the diameter of the designed wheel is 130 mm, the strength of the whole mobile mechanism part is very large. According to the vertical direction of the wheel force and the horizontal direction of the force size, it can be seen that this wheel can fully meet the design requirements.

Selection of Robot's Positioning Device on the Inner Wall of a Vertical Duct

There are three main types of positioning for vertical duct cleaning robots: vacuum adsorption, magnetic adsorption, and negative airflow adsorption [15]. Negative pressure airflow adsorption will cause dust to be generated during the cleaning operation, affecting the observation of the camera device, and is not suitable for cleaning the inner wall of central air conditioning ducts. Therefore, the following focuses on the analysis of vacuum adsorption and magnetic adsorption.

Magnetic adsorption is the process of allowing the robot to adhere to the inner wall of the duct through magnetic force. However, magnetic adsorption has great limitations on the materials of the usage environment. This article focuses on the vertical air duct wall of central air conditioners. Since there is no unified material standard for domestically produced air ducts, the scope of application is not as large as vacuum adsorption, and the manufacturing price is higher than that of suction cups, so suction cups are chosen as the positioning device of the cleaning robot in this article.

Most vacuum adsorption uses a suction cup as an adsorption device, and the air inside the suction cup is expelled by squeezing or pumping to achieve the adsorption function. Among them, vacuum adsorption is the most widely used, and has little restriction on the materials used, and can adapt to most working environments. Therefore, this paper selects the suction cup as the adsorption and positioning device of the cleaning robot, and Figure 5 is a wheel suction cup assembly.

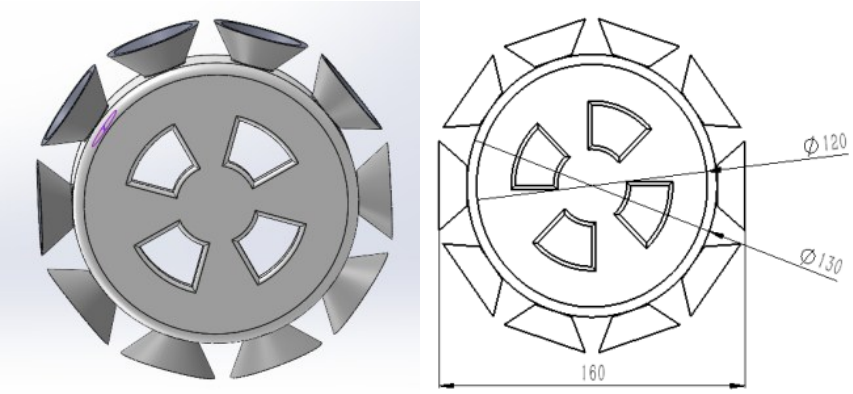

Fig. 5. Wheel suction cups

Design of the Cleaning Mechanism

The cleaning mechanism mainly consists of a mechanical arm, a flexible arm, and a brush connected to the flexible arm. When working, as the robot moves forward, the flexible arm starts to rotate at high speed, and the brush connected to the arm also rotates with the rotation of the flexible arm. As the mechanical arm gradually adjusts to the working height, the robot begins to clean the inner wall.

Rotary Brush Drive Motor Selection

When the robot is working, the high-speed rotation of the cleaning mechanism causes friction between the bristles and the inner wall, thus generating a large resistance torque. Therefore, we need to select a suitable drive motor in the cleaning mechanism. Figure 6 shows the schematic diagram of the rotating brush.

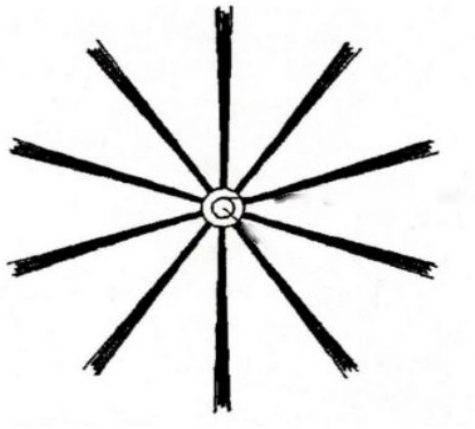

Fig. 6. Schematic diagram of rotating brush

Brush rotation torque Ma: (F is the stabilized drive wheel during operation, R is the radius of the brush shaft)

$$\boldsymbol{Ma = F \times R = Ta} \quad \text{Eq. 14}$$

Drive motor output torque Ta:

$$\boldsymbol{Ta = F \times R = 0.5\ N \cdot m} \quad \text{Eq. 15}$$

In order to ensure that the cleaning requirements, according to the actual situation to choose the speed of n=1000r/min drive motor, then the motor power is:

$$\boldsymbol{P = \frac{Ta}{9550} = 52.4W} \quad \text{Eq. 16}$$

In actual situations, due to the influence of the working environment, the motor will lose some power during the transmission process. Therefore, the power of the motor should be greater than 52.4 W to meet the work of the cleaning brush. After checking the table, a DC motor with a rated voltage of 24 V, a rated speed of 3000 r/min, and a rated power of 63 W was selected as the driving motor of the cleaning brush head.

Selection of Bristle Material

(1) Vegetable type: Not wear-resistant and easily broken, short life span, need frequent replacement, difficult to clean.

(2) Animal: Bristles made from the ends of animal hairs have good stiffness and good water resistance and service life. However, for the cleaning robot proposed in this article, this material is expensive, which is not conducive to the popularization and promotion of the robot.

(3) Metal: Bristles made of steel, copper and other materials are prone to falling off, breaking and even being greatly deformed by high temperatures during use, affecting their normal working state.

(4) Engineering plastics: With the continuous advancement of technology, engineering plastic products have become more and more advantageous in terms of

performance and price. For example, nylon material is a commonly used cleaning material [16].

Table 1. Comparison Table of Bristle Material Properties

Material name	Temperature resistance	Water resistance	Chemical stability	Dissociation	Rigidity
Nylon 6	weak	usual	usual	usual	favorable
Nylon 66	usual	weak	favorable	usual	favorable
Nylon 610	usual	talented	weak	favorable	favorable
Nylon 1010	weak	usual	usual	favorable	usual
MC Nylon	usual	favorable	favorable	favorable	talented

The bristle material chosen for the cleaning robot in this paper is MC nylon material, which is also known as cast nylon (Table 1). MC nylon has good overall advantages among nylon materials.

Design of Camera Lighting Device for Cleaning Robot

The interior of the central air conditioning system is dimly lit, and additional lighting and video equipment must be installed to facilitate operators to adjust the movements of the cleaning robot in a timely manner (Figure 7). Before cleaning, the angle of the camera and the height of the camera are adjusted to ensure that there is the best observation angle between the width range of > 400mm and the height range of 50 to 800 mm [17].

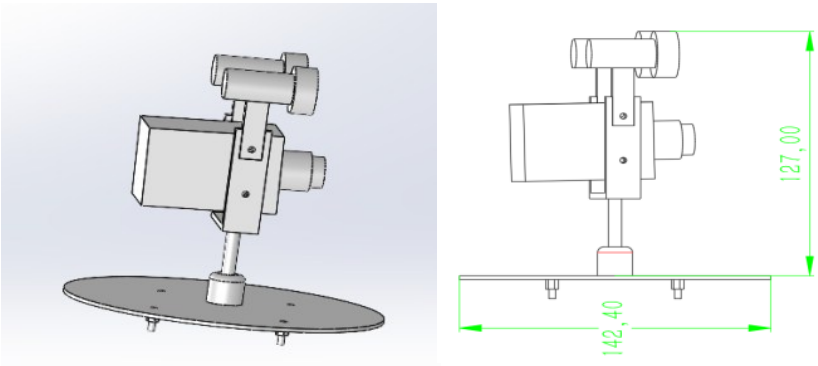

Fig. 7. Camera-illuminated device

Solar Power Plant Design

Solar panels are a type of power generation element that utilizes the photovoltaic effect. They are composed of multiple P-type semiconductors and N-type semiconductors. When sunlight shines on a semiconductor, photons excite the electron energy state inside the semiconductor into electrons and holes. Under the influence of the internal electric field, holes move toward the P-type semiconductor and electrons move toward the N-type semiconductor. In this way, the P-type semiconductor generates positive electricity and the N-type semiconductor generates negative electricity. Connecting the P-type

semiconductor and the N-type semiconductor can generate direct current (DC). Figure 8 is a schematic diagram of a solar cell.

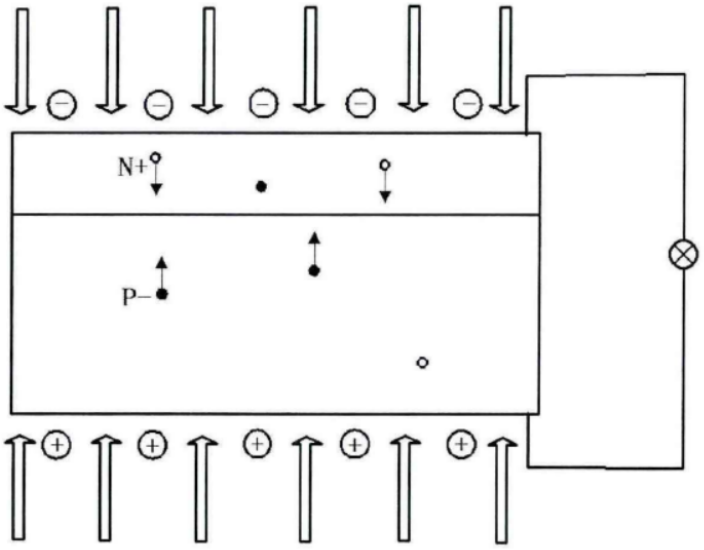

Fig. 8. Solar cell schematic diagram

2D Mapping of Cleaning Robots

Suction Pads

AutoCAD 2020 was used to draw the suction cup part (Figure 9). The suction cup part is an important element to ensure that the cleaning robot can move forward and position itself properly in the vertical duct, which is a core part of the design. Vacuum adsorption is used to achieve the positioning of the vertical duct cleaning robot when it moves in the vertical duct.

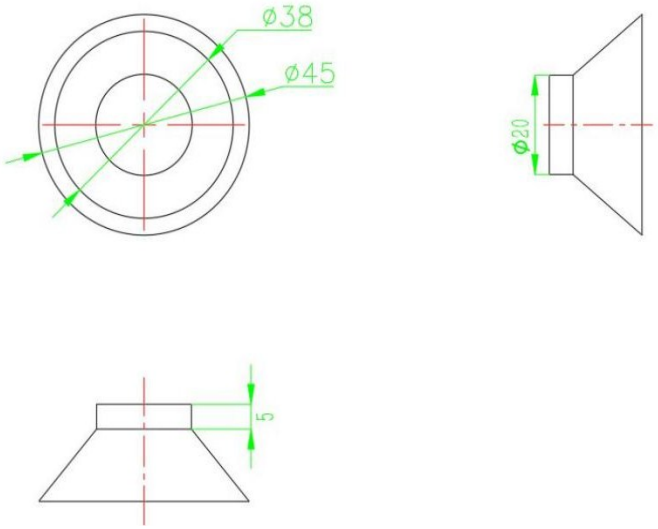

Fig. 9. 2D view of suction cup parts

Bottom Support Plate

AutoCAD 2020 was used to draw the bottom support plate with an overall size of 211 mm × 35 mm × 3 mm (Figure 10). The bottom support plate is one of the most basic components of the mobile mechanism. Together with other connecting plates and supports, it constitutes the mobile bearing part of the cleaning robot.

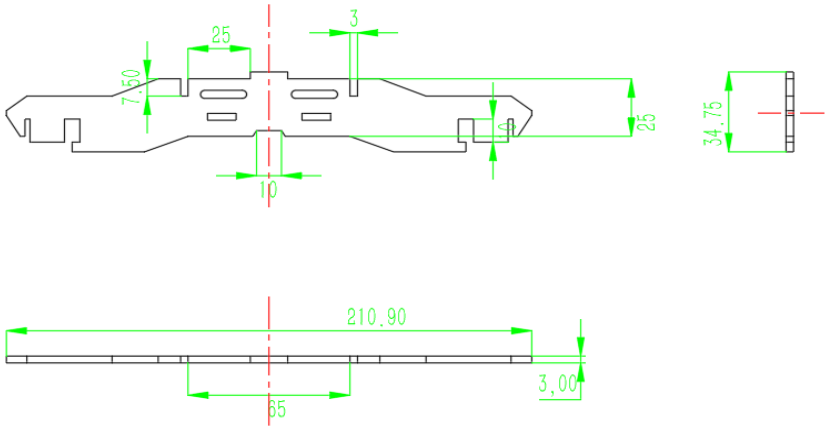

Fig. 10. 2D view of bottom support plate

Wheel

AutoCAD 2020 was used to draw the wheel parts with a radius of 75 mm and a width of 50 mm (Figure 11). The wheels of the vertical duct cleaning robot serve many purposes to beautify the appearance and make the cleaning robot more ornamental, while the suction cup positioning device of the vertical duct is also embodied in the wheels.

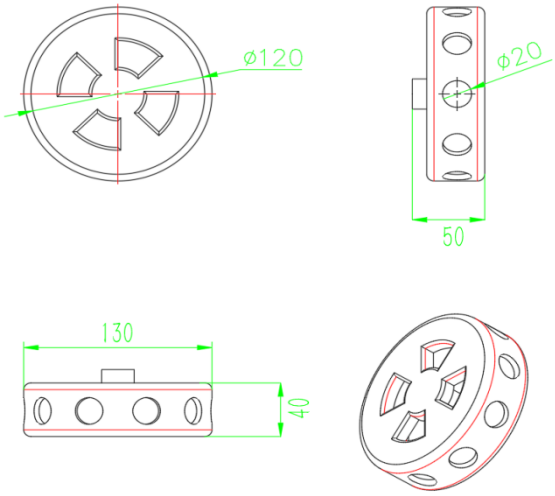

Fig. 11. Wheel 2D drawing

Cleaning Mechanism Connection

Use AutoCAD 2020 to draw a 2D drawing of the cleaning mechanism connection with a diameter of 40 mm (Figure 12). The connecting knot is crucial in the cleaning mechanism as it connects the flexible arm and the brush extending from the flexible arm.

The connection knot can make the flexible arm move more stably and complete the cleaning task more effectively.

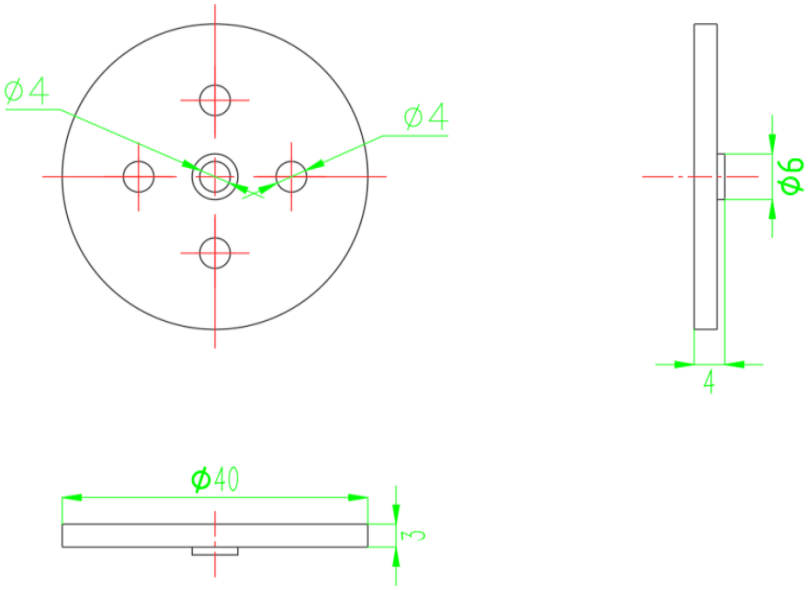

Fig. 12. 2D diagram of the connection junction of the cleaning mechanism

Cleaning Mechanism Swivel Connector

Use AutoCAD 2020 to draw a 2D drawing of the rotary connector of the cleaning mechanism with dimensions of 30 mm × 30 mm × 4 mm (Figure 13). The rotary connector is an important part of the cleaning mechanism that connects the motor to rotate the cleaning flexible arm.

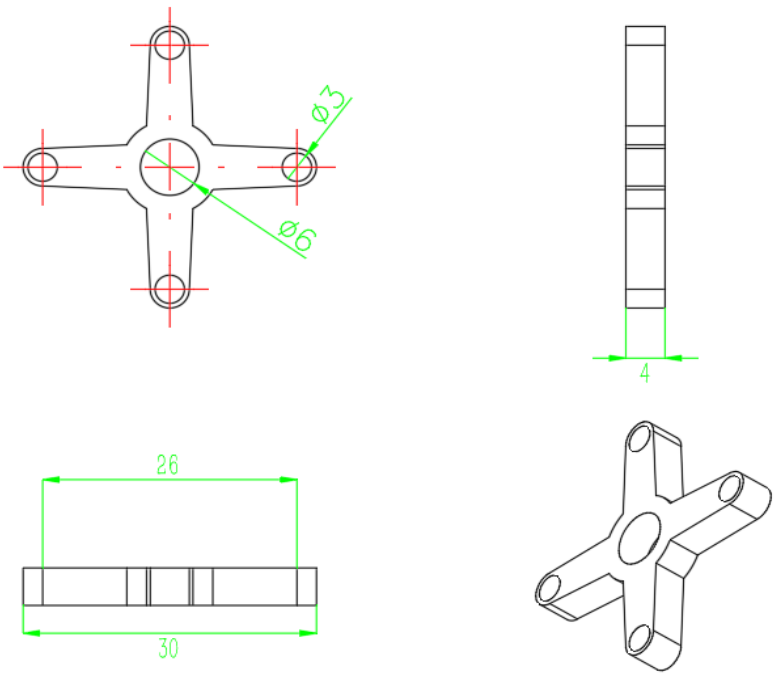

Fig. 13. 2D drawing of rotary joints

2D Drawing of the Mobile Mechanism

The 2D drawing of the mobile part of the cleaning robot with dimensions of 380mm×300mm×160mm using AutoCAD 2020 is shown in Figure 14. The mobile mechanism plays an important role in the whole cleaning robot to support the cleaning robot to complete the work and provide power to the cleaning robot.

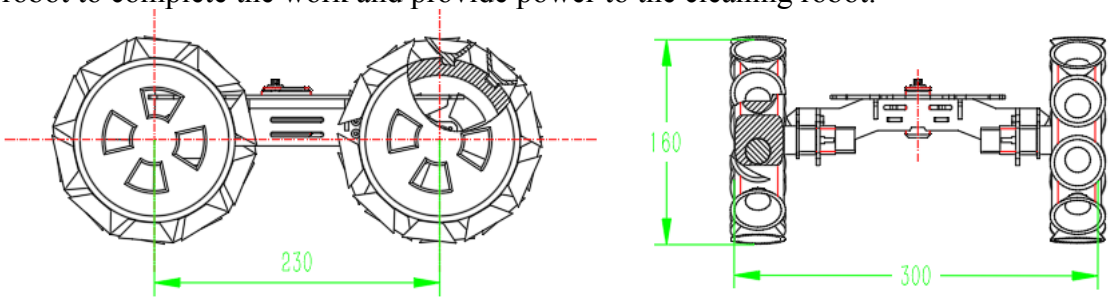

Fig. 14. Moving mechanism partially assembled

2D Drawing of the Cleaning Mechanism

AutoCAD2020 was used to draw a two-dimensional drawing of the cleaning mechanism with dimensions of 205 mm × 40 mm × 40 mm as shown in Figure 15. The cleaning mechanism is driven by a DC motor, which drives the connected steel wire rope to rotate the bristles at high speed to achieve the purpose of cleaning the inner wall of the air duct.

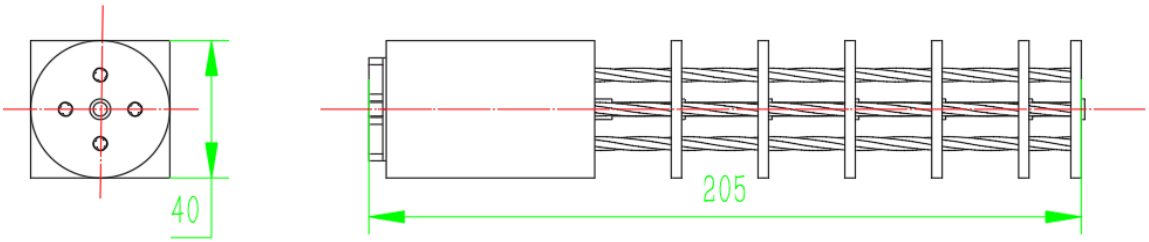

Fig. 15. Cleaning mechanism partially assembled

2D Drawing of a Solar Installation

AutoCAD 2020 was utilized to draw a two-dimensional drawing of the solar device with dimensions of 150 mm × 112 mm × 152 mm, as shown in Figure 16.

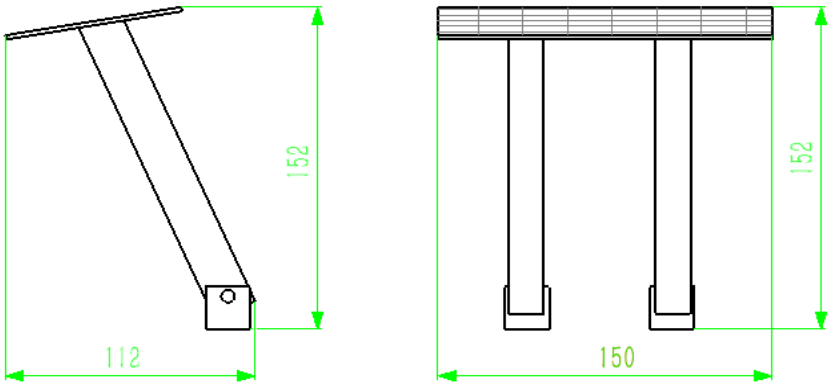

Fig. 16. Partial Installation Diagram of Solar System

General Assembly Drawing of Cleaning Robot

AutoCAD 2020 was used to draw the two-dimensional assembly drawing of the cleaning robot, with an overall dimension of 562 mm × 296 mm × 427 mm, as shown in Figure 17. The overall cleaning robot is composed of four main parts: the mobile plate, cleaning plate, camera, support plate and arm connection plate. The plate thickness is basically 2mm or 3mm, and the material is No. 45 steel. The cleaning mechanism is MC nylon bristles, and the camera device is a CCD camera device. Before working, adjust the height of the camera to have the best working field. Then, driven by the mobile device, the cleaning robot moves forward, and the high-speed rotating cleaning brush is used to clean the central air-conditioning vertical ventilation ducts with a size range of 400mm wide and a height range of 500 mm to 800 mm.

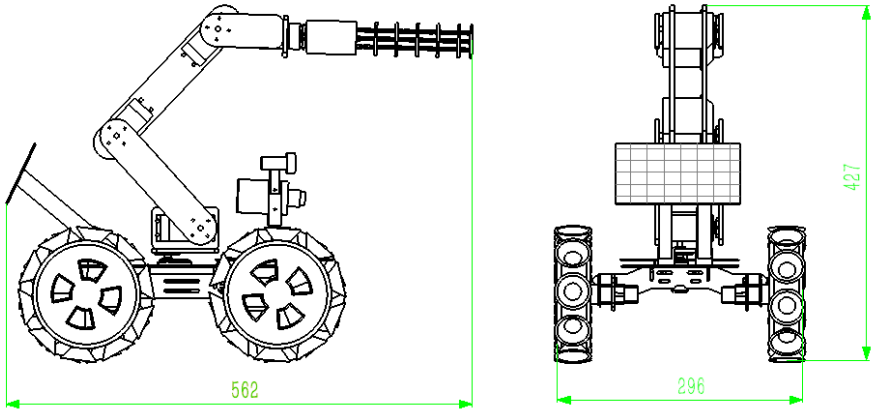

Fig. 17. General assembly diagram of cleaning robot

3D Parts Modeling

Suction Cup

The suction cup part was modeled using SolidWorks 2021 and the modeling result is shown in Figure 18.

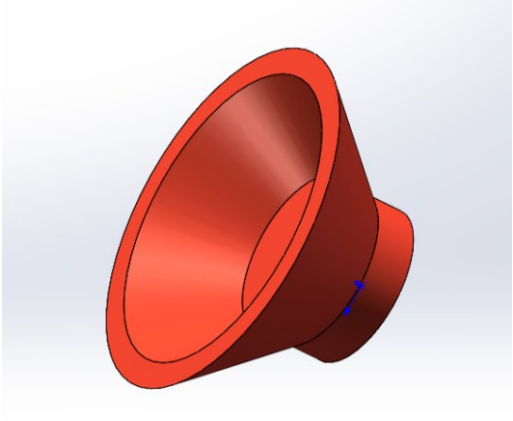

Fig. 18. 3D model of suction cup parts

Wheel Modeling

The wheel part was modeled using SolidWorks 2021 and the modeling result is shown in Figure 19.

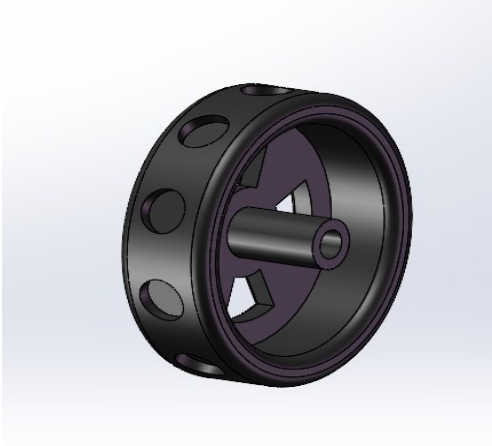

Fig. 19. 3D model of wheel parts

Cleaning Mechanism Wire Rope Modeling

The cleaning mechanism wire rope was modeled using SolidWorks 2021 and the result is shown in Figure 20.

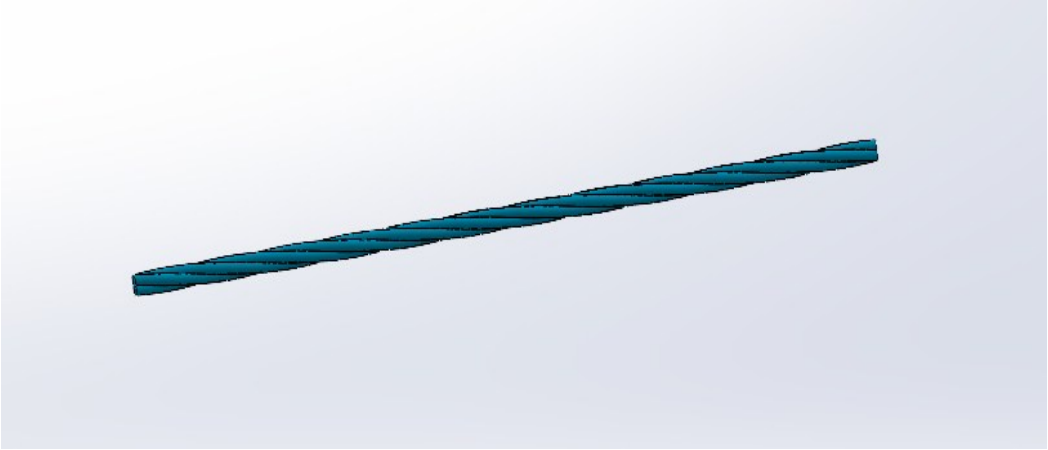

Fig. 20. 3D model of a wire rope

Assembly Drawing of Moving Mechanism

The moving mechanism was assembled using SolidWorks 2021 and the results are shown in Figure 21.

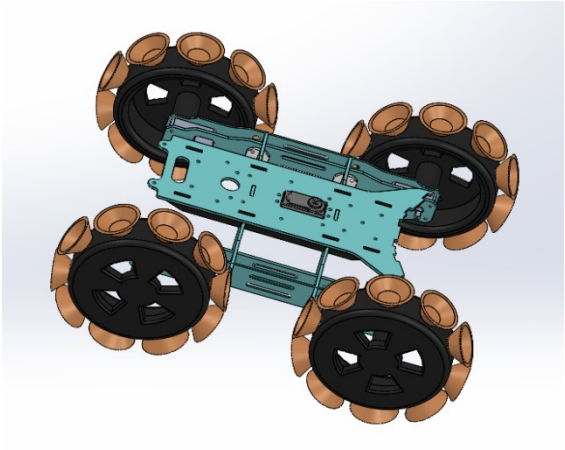

Fig. 21. Mobile mechanism assembly drawing

Cleaning Mechanism Assembly Diagram

The cleaning mechanism was assembled using SolidWorks 2021 and the results are shown in Figure 22.

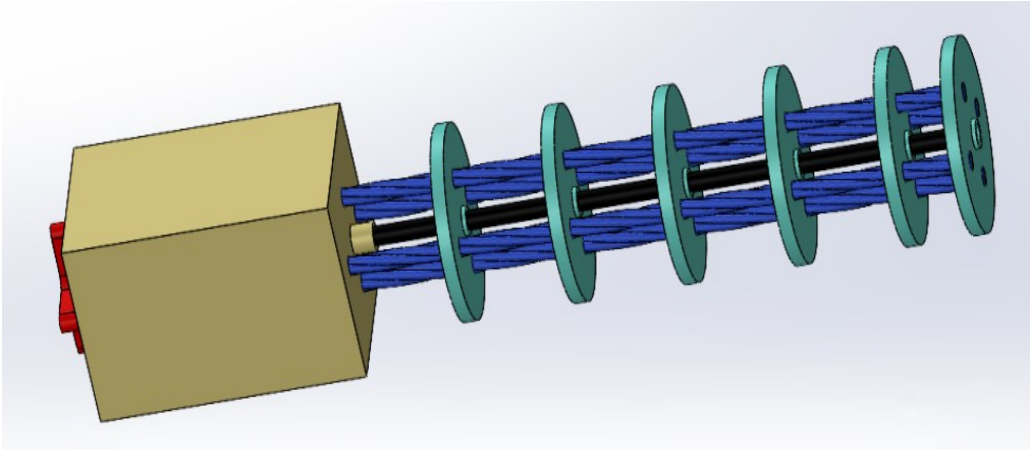

Fig. 22. General assembly drawing of the cleaning mechanism

Camera Lighting Unit Assembly Diagram

The camera lighting unit was assembled using SolidWorks 2021 and the results are shown in Figure 23.

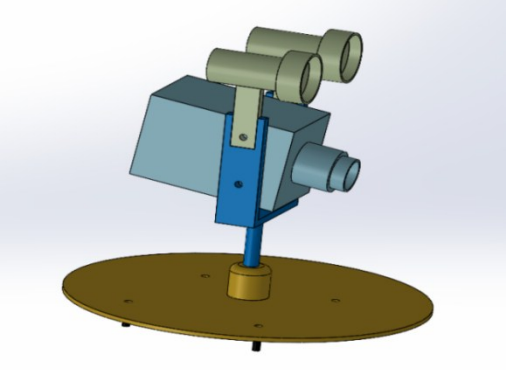

Fig. 23. Camera lighting unit general assembly drawing

Solar Unit Assembly Diagram

The solar unit was assembled using SolidWorks 2021 and the results are shown in Figure 24.

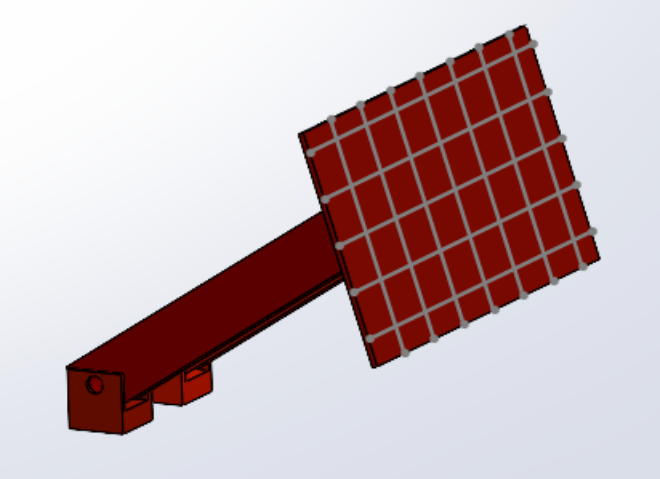

Fig. 24. Solar Unit Assembly Diagram

General Assembly Diagram of Vertical Duct Cleaning Robot

Using SolidWorks 2021, the moving, cleaning, camera parts and solar unit were assembled, resulting in an overall assembly drawing of the cleaning robot (Figure 25)

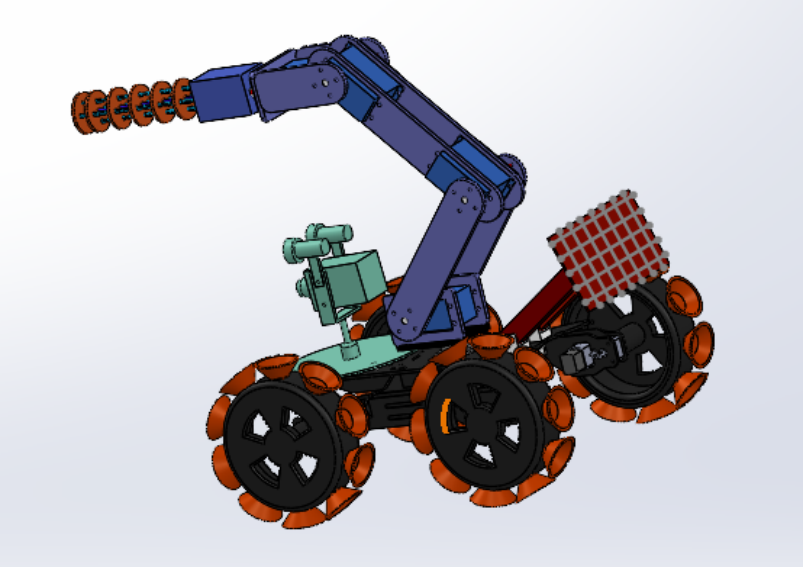

Fig. 25. General assembly drawing of cleaning robot

CONCLUSIONS

This paper mainly carries out the selection of driving mode and the calculation of driving motor types for the cleaning mechanism and the moving mechanism, and selects 63 W, 24 V and 30 W, 24 V DC motors, respectively. The cleaning brush type and the camera lighting device type are selected as MC nylon brush and CCD camera device respectively, and a three-dimensional configuration diagram of the solar device is attached. Finally, the dimensions of each part of the cleaning robot are determined according to the range of vertical ducts to be cleaned. AutoCAD 2020 was used to draw

the 2D drawings and assembly drawings of the important components, while SolidWorks 2021 was used for 3D modeling and assembly of the designed vertical duct cleaning robot.

Based on the literature, the following suggestions are made for future research on cleaning robots: 1. The current cleaning robots need to be further optimized in terms of obstacle avoidance ability and adaptability to the cleaning environment. 2. The current cleaning robot cleaning method is too single, need to be optimized accordingly. 3. The control system of the cleaning robot still needs to be developed.

CONFLICTS OF INTEREST

The author declares that there is no conflict of interests regarding the publication of this paper.

REFERENCES

[1] Sawadogo, W., Abiodun, B. J., & Okogbue, E. C. (2020). Impacts of global warming on photovoltaic power generation over West Africa. *Renewable Energy, 151*, 263-277. doi: https://doi.org/10.1016/j.renene.2019.11.032

[2] Baloch, M. H., Tahir Chauhdary, S., Ishak, D., Kaloi, G. S., Nadeem, M. H., Wattoo, W. A., Younas, T., & Hamid, H. T. (2019). Hybrid energy sources status of Pakistan: An optimal technical proposal to solve the power crises issues. *Energy Strategy Reviews, 24*, 132-153. doi: https://doi.org/10.1016/j.esr.2019.02.001

[3] Gorjian, S., Minaei, S., MalehMirchegini, L., Trommsdorff, M., & Shamshiri, R. R. (2020). Chapter 7 - Applications of solar PV systems in agricultural automation and robotics. In S. Gorjian & A. Shukla (Eds.), *Photovoltaic Solar Energy Conversion* (pp. 191-235): Academic Press

[4] Ahmed, S., Zenan, A. H., & Rahman, M. (2014). *A two-seater light-weight solar powered clean car: Preliminary design and economic analysis.* Paper presented at the 2014 3rd International Conference on the Developments in Renewable Energy Technology (ICDRET). doi: https://doi.org/10.1109/ICDRET.2014.6861646

[5] Alhammad, Y. A., & Al-Azzawi, W. F. (2015, 8-10 Dec. 2015). *Exploitation the waste energy in hybrid cars to improve the efficiency of solar cell panel as an auxiliary power supply.* Paper presented at the 2015 10th International Symposium on Mechatronics and its Applications (ISMA). doi: https://doi.org/10.1109/ISMA.2015.7373466

[6] Tang, J., Ye, B., Lu, Q., Wang, D., & Li, J. (2013). Economic Analysis of Photovoltaic Electricity Supply for an Electric Vehicle Fleet in Shenzhen, China. *International Journal of Sustainable Transportation,* 8(3), 202–224. doi: https://doi.org/10.1080/15568318.2012.665980.

[7] Selin, I. A. (2023). New methods for efficient energy management of a solar vehicle on a fixed route. *Информатика, телекоммуникации и управление*, *16*(4), 18-27. doi: https://doi.org/10.18721/JCSTCS.16402

[8] Yao, Y., & Chen, J. (2010). Global optimization of a central air-conditioning system using decomposition–coordination method. *Energy and Buildings, 42*(5), 570-583. doi: https://doi.org/10.1016/j.enbuild.2009.10.027

[9] Absar Alam, M., Kumar, R., Yadav, A. S., Arya, R. K., & Singh, V. P. (2023). Recent developments trends in HVAC (heating, ventilation, and air-conditioning) systems: A comprehensive review. *Materials Today: Proceedings*. doi: https://doi.org/10.1016/j.matpr.2023.01.357

[10] Dai, M., Li, H., & Wang, S. (2023). A reinforcement learning-enabled iterative learning control strategy of air-conditioning systems for building energy saving by shortening the morning start period. *Applied Energy, 334*, 120650. doi: https://doi.org/10.1016/j.apenergy.2023.120650

[11] Ismail, M., Zahra, W. K., & Hassan, H. (2023). Numerical investigation of the air conditioning system performance assisted with energy storage of capsulated concave/convex phase change material. *Journal of Energy Storage, 68*, 107651. doi: https://doi.org/10.1016/j.est.2023.107651

[12] Wang, Y., & Zhang, J. (2006, 6-9 Aug. 2006). *Autonomous Air Duct Cleaning Robot System.* Paper presented at the 2006 49th IEEE International Midwest Symposium on Circuits and Systems. doi: https://doi.org/10.1109/MWSCAS.2006.382110

[13] Yan, H., Niu, H., Chang, Q., Zhao, P., & He, B. (2024). Study on Dynamic Characteristics of Pipeline Jet Cleaning Robot. *13*(2), 49. doi: https://doi.org/10.3390/act13020049

[14] Li, Y., Ye, S., Cui, R., & Shou, Z. (2024). The Design and Analysis of a Tunnel Retro-Reflective Ring Climbing and Cleaning Robot. *13*(6), 197. doi: https://doi.org/10.3390/act13060197

[15] Li, X. P., Wang, X., & Feng, B. (2021). Modeling and control of a novel facade cleaning robot with four-ducted fan drive. *International Journal of Advanced Robotic Systems, 18(*3), 1729881420985721. doi: https://doi.org/10.1177/1729881420985721

[16] Ballini, A., Di Cosola, M., Saini, R., Benincasa, C., Aiello, E., Marrelli, B., Rajiv Saini, S., Ceruso, F. M., Nocini, R., Topi, S., Bottalico, L., Pettini, F., & Cantore, S. (2021). A Comparison of Manual Nylon Bristle Toothbrushes versus Thermoplastic Elastomer Toothbrushes in Terms of Cleaning Efficacy and the Biological Potential Role on Gingival Health. *11*(16), 7180. doi: https://doi.org/10.3390/app11167180

[17] Duan, K., Suen, C. W. K., & Zou, Z. (2023). Robot morphology evolution for automated HVAC system inspections using graph heuristic search and reinforcement learning. *Automation in Construction, 153*, 104956. doi: https://doi.org/10.1016/j.autcon.2023.104956